Solid State Communications 236 (2016) 32–36

Contents lists available at ScienceDirect

Solid State Communications

journal homepage: www.elsevier.com/locate/ssc

Soft X-ray absorption and photoemission spectroscopy study of semiconductor oxide nanoparticles for dye-sensitized solar cell: $ZnSnO_3$ and Zn_2SnO_4

Hyun Woo Kim [a], Eunsook Lee [a], D.H. Kim [a], Seungho Seong [a], Soo Yeon Moon [b], Yu-Ju Shin [b], J. Baik [c], H.J. Shin [c], J.-S. Kang [a,*]

[a] Department of Physics, The Catholic University of Korea (CUK), Bucheon 14662, South Korea
[b] Department of Chemistry, The Catholic University of Korea (CUK), Bucheon 14662, South Korea
[c] Pohang Accelerator Laboratory (PAL), POSTECH, Pohang 37673, South Korea

ARTICLE INFO

Article history:
Received 21 January 2016
Received in revised form
2 March 2016
Accepted 15 March 2016
by X.C. Shen
Available online 19 March 2016

Keywords:
A. Solar cell
D. Electronic structure
E. XAS
E. PES

ABSTRACT

The electronic structures of the Zn-stannate nanoparticles of $ZnSnO_3$ and Zn_2SnO_4, which are the potential nano-structured semiconductor oxides for a dye sensitized solar cell (DSSC), have been investigated by employing photoemission spectroscopy (PES) and soft X-ray absorption spectroscopy (XAS), and compared to those of reference materials. The divalent and tetravalent valence states of Zn^{2+} and Sn^{4+} ions are confirmed experimentally. The energy levels of both the valence-band and conduction-band edges are determined experimentally. The top of the valence band in PES is slightly higher in Zn_2SnO_4 than in $ZnSnO_3$. The onset energies of the O 1*s* XAS spectra of the Zn-stannates are found to be similar to each other, but higher than that of TiO_2. The O 1*s* XAS spectrum of $ZnSnO_3$ exhibits the higher unoccupied density of states near the bottom of the conduction band than those of Zn_2SnO_4, SnO_2 and ZnO, reflecting the larger number of holes in the Zn 3*d* bands of $ZnSnO_3$. Hence, the easier electron transfer is expected from the LUMO (lowest unoccupied molecular orbital) of a dye molecule to the conduction band of $ZnSnO_3$ nanoparticles on the transparent conductive electrode of a DSSC.

1. Introduction

The solar cell research has become very active due to the energy problems, and the dye-sensitized solar cell (DSSC) is considered to be one of the best candidates [1–5]. As shown in Fig. 1 for the operation of a DSSC [1,3,6,7], a nano-structured semiconductor oxide (called as the "NSO" hereafter) film, covered with a monolayer of sensitizing dye, is deposited on a transparent conductive electrode (TCE). The small energy separation (ΔE_{dye}) between the highest occupied molecular orbital (HOMO) and the lowest unoccupied molecular orbital (LUMO) of the dye molecule ensures the absorption of low-energy photons. Then the maximum potential (V_{OC}) produced by a DSSC is determined by the Fermi level (E_F) of the NSO and the chemical potential of the electrolyte (E_{redox}). The efficiency of a DSSC depends on the relative energy levels between the LUMO level of the dye molecule and the E_F of the NSO. The increased energy separation (ΔE_{LC}) between the LUMO level and the bottom of the conduction band (E_{CB}) of the NSO will improve the effective electron injection from the LUMO level to the conduction band of the NSO [8]. Hence, ΔE_{LC} is an important factor that determines the electron current in a DSSC.

Recently a novel polar $LiNbO_3$ (LN)-type oxide of $ZnSnO_3$ (see Fig. 2(a)) has been prepared successfully by high-pressure synthesis [9]. Under normal pressure, $ZnSnO_3$ crystallizes in the ilmenite (IL)-type structure (see Fig. 2(b)) [10]. Electronic structure calculations for two types of $ZnSnO_3$ show that the LN-type structure is more stable than the IL-type structure [11,12]. Another recent calculation on the electronic structure and the optical properties of *n*-type doped $ZnSnO_3$ [13] suggests that the *n*-type doped $ZnSnO_3$ with a LN-type structure is very promising as a high-performance transparent conducting oxide (TCO) material in solar photovoltaics.

There exists another phase of the Zn-stannate, a spinel-type Zn_2SnO_4 (see Fig. 2(c)). The successful synthesis of high-yield, uniform, and band-gap tunable Zn_2SnO_4 nanocube-based films has been reported [14]. These band-gap tunable Zn_2SnO_4

* Corresponding author at: Department of Physics, The Catholic University of Korea, Korea.
E-mail addresses: hyoow349@naver.com (H.W. Kim), lizzero7@gmail.com (E. Lee), rnb000@gmail.com (D.H. Kim), sht125@naver.com (S. Seong), msy0609@catholic.ac.kr (S.Y. Moon), yujushin@catholic.ac.kr (Y.-J. Shin), cla100@postech.ac.kr (J. Baik), shj001@postech.ac.kr (H.J. Shin), kangjs@catholic.ac.kr (J.-S. Kang).

http://dx.doi.org/10.1016/j.ssc.2016.03.011
0038-1098/

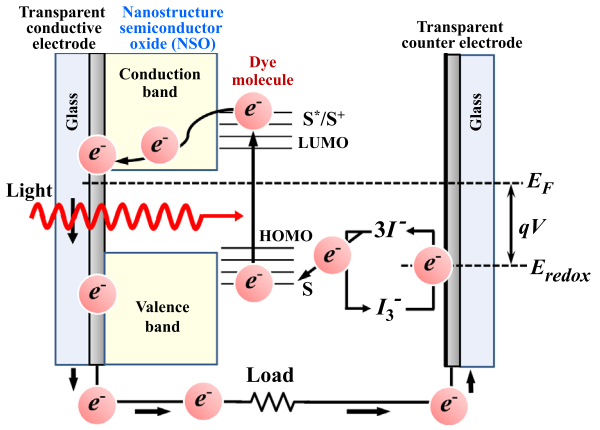

Fig. 1. (Color online) Schematic diagram of the operation principle of dye sensitized solar cell (DSSC). In this work, $ZnSnO_3$ and Zn_2SnO_4 are studied as candidate nano-structured semiconductor oxide (NSO) films on a transparent conductive electrode (TCE) depicted in grey.

nanocube-based films exhibit high photo-current and the large photocurrent-to-dark current ratio, which are very valuable for a high-performance DSSC. Indeed, promising physical properties were observed in Zn_2SnO_4 nanoparticles as a DSSC [15]. The pressure dependence of the band structures, energy gap, and density of states (DOS) in Zn_2SnO_4 were investigated theoretically [16].

The NSO that has a lower E_{CB} would be more promising for a DSSC since the LUMO and HOMO energy levels are fixed for a given dye molecule. The energy gaps of Zn-stannate nanoparticles of $ZnSnO_3$ and Zn_2SnO_4 were measured by employing UV absorption spectroscopy [17]. However, the energy levels of their conduction-band (CB) edges have not been measured so far. Therefore it is important to determine the E_{CB} levels of the potential NSO nanoparticles experimentally. For this purpose, soft X-ray absorption spectroscopy (XAS) [18,19], in particular O 1*s* (*K*-edge) XAS, is a very powerful experimental method because O 1*s* XAS allows us to measure the unoccupied CB DOS of the oxides [20,21].

In this work, we have investigated the electronic structures of the potential candidate nano-structured semiconductor oxides for DSSC, such as $ZnSnO_3$ and inverse spinel Zn_2SnO_4 nanoparticles, as well as SnO_2, ZnO, and TiO_2 as reference NSOs, by employing photoemission spectroscopy (PES) and XAS. PES allows one to observe experimentally the occupied part of the electronic structures [22], while O 1*s* XAS represents the unoccupied DOS of the conduction-band electronic states via hybridization to the O 2*p* states [20,21,23]. The novelty of this work is that the energy levels of both the VB edges and the CB edges are determined experimentally. All the samples were mounted on the same holder and measured under the same experimental conditions. Hence the relative energy positions of both the top of the valence band and the bottom of the conduction band, determined in this work, are very reliable.

2. Experimental details

High-quality polycrystalline semiconductor nanoparticles were synthesized. For nanocrystalline SnO_2 powder, a commercial SnO_2 aqueous colloid (Alfa Aesar; 4–5 nm, 15% in water) was used after evaporating water. The ZnO particles were prepared using a modified sol-gel method [24], where the water content was carefully controlled [25]. Zn_2SnO_4 was prepared from the hydrothermal reaction of $Zn(CH_3COO)_2 \cdot 2\,H_2O$ and $SnCl_4 \cdot 2\,H_2O$ with NaOH as mineralizer at 170 °C [26].

$ZnSnO_3$ was prepared using a precursor Li_2SnO_3 following a modified ion-exchange reaction proposed by Kovacheva [27]. First, Li_2SnO_3 was prepared by a solid state reaction with Li_2CO_3, by the following equation:

$$SnO_2(s) + Li_2CO_3(s) \rightarrow Li_2SnO_3(s) + CO_2(g)\uparrow \quad (1)$$

In this reaction, about 10% excess of Li_2CO_3 was used for volatility and the mixture was heated at 450 °C for 4–5 h and then at 1000 °C for 8 h. The product was washed with distilled water and ethanol to remove the excessive lithium component and dried at 70 °C. Then as-prepared Li_2SnO_3 was mixed with KNO_3 and $ZnCl_2$ with a weight ratio of 1:8:6 and then put into a pyrex tube, which was sealed under vacuum (< 1 Torr) and heated at 300 °C for 14 days to carry out by the following equation:

$$Li_2SnO_3(s) + ZnCl_2(l) \rightarrow ZnSnO_3(s) + 2LiCl_2(l). \quad (2)$$

The excess salts were removed by washing out with distilled water and 0.1 M HCl aqueous solution for several times. White product of $ZnSnO_3$ was finally recovered by rinsing out the HCl solution with distilled water and ethanol followed by drying at 70 °C. Particle sizes [25,28] are about ~10 nm for SnO_2, 50–100 nm for ZnO, 30–100 nm for Zn_2SnO_4, and 200–700 nm for $ZnSnO_3$.

The measured XRD (X-ray diffraction) patterns and SEM (scanning electron microscopy) images of $ZnSnO_3$ and Zn_2SnO_4 are shown in Fig. 2(d)–(g). These XRD data confirm that $ZnSnO_3$ and Zn_2SnO_4 samples have the single-phase IL and inverse spinel structures, respectively, without having detectable impurity phases. SEM images show that these samples are nanoparticles and that the particle sizes of Zn_2SnO_4 are smaller than those of $ZnSnO_3$. Further, the Zn_2SnO_4 particles exhibit the polygon-type features (similar to octahedral shapes), while the $ZnSnO_3$ particles have the rounded shapes. These differences are similar to those observed in Zn-stannate single crystals [17].

PES and XAS measurements were performed at the 8A1 beam line of the Pohang Light Source (PLS). PES and XAS data were obtained at room temperature under the base pressure less than 3×10^{-10} Torr. XAS data were obtained by employing the total electron yield mode with the photon energy ($h\nu$) resolution of ~100 meV at $h\nu \approx 500$ eV. All the samples were mounted on the same holder and measured at the same beamline under the same experimental conditions. The Fermi level E_F and the instrumental resolution of the system were determined from the near-E_F spectrum of Au metal in electrical contact with samples [29]. The overall instrumental resolution of the PES spectra was about ~0.3 eV at $h\nu \sim 500$ eV. All the XAS and PES spectra were normalized to the incident photon flux.

3. Results and discussion

Fig. 3(a) and (b) shows Zn 2*p* and Sn 3*d* core-level PES spectra of $ZnSnO_3$ and Zn_2SnO_4, respectively, in comparison to those of the reference materials, which are obtained with $h\nu = 1486.6$ eV. Our core-level PES data for $ZnSnO_3$ and Zn_2SnO_4 are similar to those in Refs. [30,31]. It is observed clearly that Zn 2*p* and Sn 3*d* spectra of $ZnSnO_3$ and Zn_2SnO_4 are very similar to those of ZnO and SnO_2, respectively, indicating that Zn ions are divalent (Zn^{2+}) and Sn ions are tetravalent (Sn^{4+}) in both $ZnSnO_3$ and Zn_2SnO_4.

Fig. 3(c) shows the wide valence-band (VB) PES spectra of $ZnSnO_3$ and Zn_2SnO_4, SnO_2, ZnO, and TiO_2, obtained with $h\nu \approx 650$ eV. The large peak around ~11 eV binding energy (BE), which is absent in SnO_2 and TiO_2, is the Zn 3*d* core-level peak. The broad feature between ~4 eV and ~9 eV BE represents the occupied O 2*p* bands, which are hybridized with the Sn 5 s/5p and Zn/Ti 4 s/4p states. Since Ti ions are nearly tetravalent (Ti^{4+}) in TiO_2, the Ti 3*d* bands of TiO_2 are almost empty (with the $3d^0$